








Imprints of multielectron polarization effects in odd-even harmonic generation from CO molecules

Hien T. Nguyen ^{1,2,3} Kim-Ngan H. Nguyen ^{4,5} Ngoc-Loan Phan ^{6,7,*} Cam-Tu Le ^{8,9,†} DinhDuy Vu ⁶
 Lan-Phuong Tran ⁷ and Van-Hoang Le ^{6,7,‡}

¹*Department of Theoretical Physics, University of Science, Ho Chi Minh City 72711, Vietnam*

²*Vietnam National University, Ho Chi Minh City 70000, Vietnam*

³*Department of Physics, Tay Nguyen University, Buon Ma Thuot City 63161, Vietnam*

⁴*Institute of Fundamental and Applied Sciences, Duy Tan University, Ho Chi Minh City 71008, Vietnam*

⁵*Faculty of Natural Sciences, Duy Tan University, Da Nang City 50000, Vietnam*

⁶*Computational Physics Laboratory K002, Ho Chi Minh City University of Education, Ho Chi Minh City 72711, Vietnam*

⁷*Department of Physics, Ho Chi Minh City University of Education, Ho Chi Minh City 72711, Vietnam*

⁸*Atomic Molecular and Optical Physics Research Group, Advanced Institute of Materials Science, Ton Duc Thang University, Ho Chi Minh City 72912, Vietnam*

⁹*Faculty of Applied Sciences, Ton Duc Thang University, Ho Chi Minh City 72912, Vietnam*



(Received 28 September 2021; revised 21 December 2021; accepted 21 January 2022; published 11 February 2022)

Dynamic core-electron polarization (DCeP) is a correction to the single-active electron (SAE) approximation by considering a response of the core electrons to the time-dependent laser field. Despite being initially construed as a perturbative correction, in some cases especially atoms and molecules with large polarizabilities, DCeP can qualitatively alter predictions produced by the bare SAE theory. In this study, we unambiguously demonstrate the nonperturbative role of DCeP in the resolved odd-even high-order harmonic generation (HHG) of the CO molecule. In particular, we find that the even-to-odd ratio, i.e., the ratio between the harmonic intensities of even order and average of the two adjacent odd orders, changes by as much as one order of magnitude when DCeP is included, making the theoretically predicted values remarkably consistent with the experimental ones. This strong manifestation allows us to verify the DCeP role in HHG by experimental data. Furthermore, our analysis of the harmonic time profile shows that this agreement is not an artifact of the numerical method but reflects relevant physics, establishing that DCeP must be incorporated into the standard framework for strong-field physics.

DOI: [10.1103/PhysRevA.105.023106](https://doi.org/10.1103/PhysRevA.105.023106)

I. INTRODUCTION

Over the past few decades, advances in intense ultrashort laser technologies have enabled unprecedented nonlinear laser-matter interactions [1–3], which motivate theoretical frameworks to evolve rapidly. The simplest model is probably the single-active electron (SAE) approximation [4–10], where the least-bound electron moves in the effective potential forming by the nuclei and frozen core electrons. However, for some atoms and molecules with large polarizabilities, this approach produces unacceptable mismatches with experimental observation, raising the question of the role of the multielectron effect [11–15]. An obvious way to improve the predictive power of the SAE theory is to relax one or several of its assumptions. Instead of assuming frozen core electrons, we allow them to dynamically respond to the external laser field; thus, the field induced by core electrons over the active electron now contains an extra time-modulated term.

In a strong laser field, core electrons are periodically shaken by the external laser field, causing the dynamic core-electron polarization (DCeP) [16]. The core-electron polarization is particularly strong for polar molecules, making them suitable platforms to study the effect of this phenomenon. Many studies demonstrate that DCeP improves the quantitative agreement with experimental measurements in many aspects, including the ionization rate [15,17–20], photoelectron distribution of above-threshold ionization (ATI) [14,15], and Coulomb-explosion image of highly charged molecules [21]. In theory, the effect can be resolved in the intensity and shape of the high-order harmonic generation (HHG) spectra [22,23], but the magnitude is too small, preventing comparison with experimental data. In this paper, we aim at a different aspect of HHG spectra, the even harmonic orders. This feature is distinctive to polar molecules, which are also known to have strong DCeP manifestation, making it a good candidate to study the signature of DCeP.

The presence of both odd and even harmonic orders is due to the symmetry breaking of the laser-molecule system [24–26] (unpolarized targets in linearly polarized laser only emit odd orders). The richer resolved odd-even spectra from polar molecules thus can be used to study various molecular properties [27–30]. Features of the resolved odd-even spectra

*Corresponding author: loanptn@hcmue.edu.vn

†lethcamtu@tdtu.edu.vn

‡hoanglv@hcmue.edu.vn

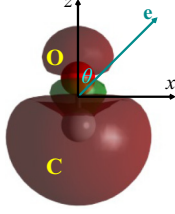


FIG. 1. The CO model and molecular frame. An electric field aligned along the unit vector \mathbf{e} makes with the molecular axis an orientation angle θ .

can be captured through the even-to-odd ratio defined as the ratio between HHG intensities of the even and the average of the two adjacent odd orders [24,25,31,32]. It is then natural to ask whether the even-to-odd ratio is sensitive to multielectron effects. Our earlier work [33] has introduced the DCEP effect on the even-to-odd ratio of fixed harmonic orders with varying CO molecular orientation. In the present work, we comprehensively investigate the imprint of the DCEP effect in the even-to-odd ratio from CO molecules exposed to a linearly polarized laser pulse. The influence is not only analyzed theoretically but also compared with the available experimental measurements [24,25]. We also establish that the strong manifestation of DCEP in the even-to-odd ratio is a consequence of the DCEP influence on the magnitude and phase of the harmonic time profile.

II. NUMERICAL METHODS

To simulate HHG, we numerically solve the time-dependent Schrödinger equation (TDSE) in the framework of SAE approximation, incorporating the DCEP potential. Although all-electron methods of time-dependent density functional theory [34] and multiconfiguration time-dependent Hartree-Fock [35] can capture multielectron dynamics, the TDSE method saves computational resources, and the roles of physical processes, particularly the DCEP, are more transparent.

The TDSE method for the system of CO molecule and a linearly polarized laser pulse is presented in detail in our previous works [23,32,33,36]. Accordingly, the potential of the CO molecule is constructed within the SAE approximation [37,38]. The SAE potential gives the 5σ energy of -0.510 a.u. in good consistency with the experimental value of -0.514 a.u. for CO [39]. The 5σ permanent dipole of 1.55 a.u. well matches 1.57 a.u. obtained by the time-dependent density functional theory [40]. For establishing the calculation, the CO molecular axis is aligned along the z axis, as exhibited in Fig. 1.

The coupling of the active electron and the time-dependent electric field is written as

$$V_L(\mathbf{r}, t) = \mathbf{r} \cdot \mathbf{E}(t), \quad (1)$$

where the electric field has the following form,

$$\mathbf{E}(t) = \mathbf{e} f(t) E_0 \sin(\omega_0 t + \varphi), \quad (2)$$

in which, E_0 , ω_0 , φ , and $f(t)$ are respectively the peak amplitude, carrier frequency, carrier-envelope phase, and envelope function of the laser pulse. \mathbf{e} is a unit vector located in the xz

plane, as shown in Fig. 1. The angle θ between the z axis and vector \mathbf{e} is called the orientation angle.

Besides the SAE component, we add an extra term describing the interaction between the active electron with the dynamically polarized core electrons, i.e., DCEP potential

$$V_P(t) = -\frac{\mathbf{E}(t) \hat{\alpha}_c \mathbf{r}}{r^3}. \quad (3)$$

Here, $\hat{\alpha}_c$ is the total polarization tensor of the core electrons whose values are taken from Ref. [18]. Specifically, $\alpha_{cxx} = \alpha_{cyy} = 6.72$ a.u. and $\alpha_{czz} = 12.22$ a.u. It is worth noting that within a small distance near the core, i.e., $r \leq r_c$ with $r_{cx} = r_{cy} = \alpha_{cxx}^{1/3}$ and $r_{cz} = \alpha_{czz}^{1/3}$, the polarization potential should cancel the external laser field [16,17]. Operationally, both the external and DCEP potentials are turned off at $r \leq r_c$ to avoid the singularity and also minimize the unphysical dipole coupling of the highest occupied molecular orbital (HOMO) to the lower lying bound states [20].

After getting the time-dependent wave function $\psi(\mathbf{r}, t)$ by solving the TDSE, we calculate the induced dipole acceleration as

$$\mathbf{a}(t) = \frac{d^2}{dt^2} \langle \psi(\mathbf{r}, t) | \mathbf{r} | \psi(\mathbf{r}, t) \rangle. \quad (4)$$

The HHG spectra are obtained by taking the square modulus of the Fourier transform of the acceleration dipole. We are interested in both parallel and perpendicular HHGs, i.e., whose polarization is respectively parallel and perpendicular to the external electric polarization.

To analyze the spectral and temporal behaviors of HHG, we utilize the Gabor transform with the following form,

$$A(\Omega, t) = \int dt' a(t') \frac{\exp[-(t' - t)^2 / 2\sigma^2]}{\sigma \sqrt{2\pi}} \exp(i\Omega t'), \quad (5)$$

where Ω is the harmonic frequency; $\sigma = (3\omega_0)^{-1}$ ensures the impartiality between the resolutions in the temporal and frequency domains [41]. Through this analysis, we easily obtain both the numerical amplitude and phase of the attosecond bursts from the induced dipole acceleration simulated by TDSE; see Eq. (4).

To ensure the numerical convergence for all laser parameters used in this study, we perform the calculation with 380 radial grid points and 180 B-spline functions in a spherical box within the radius of 100 a.u., 50 partial waves, and the time step of 0.055 a.u. The total basis set is $395\,213$. To prevent the artificial reflections from the grid boundary, the $\cos^{1/8}$ mask function [42] is applied at a distance beyond r_{mask} . If both the short and long trajectories are to be kept, we set $r_{\text{mask}} = 60$ a.u., which equals $3/5$ radius of the simulated box.

Throughout this study, to obtain sharp peaks at integer harmonic orders, we adopt a 10-cycle laser pulse with the trapezoidal envelope, in which two optical cycles linearly ramp up and down, and eight cycles in the flat part. We have examined for laser pulse with a larger number of optical cycles and obtained the same conclusion. The carrier-envelope phase φ is set to π .

We also consider the macroscopic propagation, which can be mimicked by selecting only short trajectories in theoretical simulations [30,43–45]. In this case, we apply the trajectory-resolved numerical procedure with restriction of the absorbing

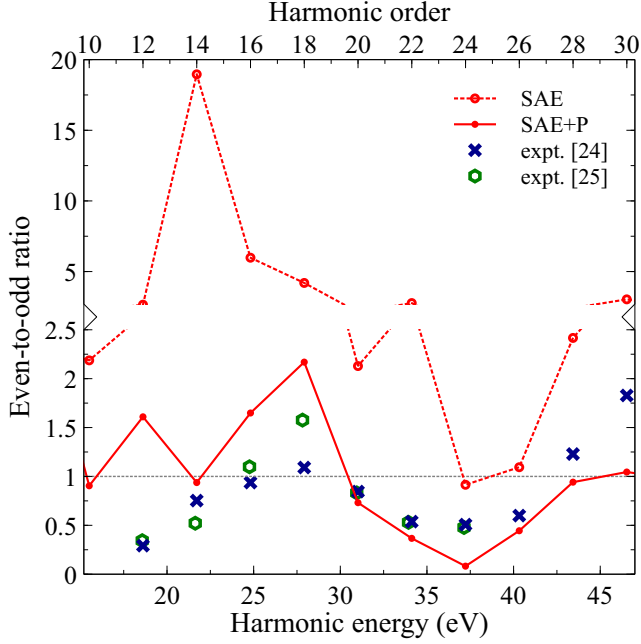


FIG. 2. The simulated even-to-odd ratios of the CO molecules with DCEP (SAE + P) (solid line) and without DCEP (SAE) (dashed line). The 800-nm laser pulse with the intensity of $1.5 \times 10^{14} \text{ W/cm}^2$ is used. The experimental data are taken from Refs. [24] (blue crosses) and [25] (green open hexagons) for the 800-nm laser pulse with intensities of $1.5 \times 10^{14} \text{ W/cm}^2$ and $2.2 \times 10^{14} \text{ W/cm}^2$, respectively. The break interval in y axis is [2.5, 2.7], dividing the figure into two spaces with different scales. The experimental even-to-odd ratios match the theoretical ones with the DCEP effect.

boundary beyond the maximal displacement of the short electron trajectories in the laser field, $r_{\text{mask}} = 1.2E_0/\omega_0^2$. As shown in numerical simulations in Appendix A, this practice indeed produces smooth even-to-odd ratios that are relatively independent of the laser parameters. Remarkably, experimental data that measured the even-to-odd ratio of CO molecule when the laser intensity of $1.5 \times 10^{14} \text{ W/cm}^2$ [24] and $2.2 \times 10^{14} \text{ W/cm}^2$ [25], as shown in Fig. 2, also exhibits stability against different laser intensities. Supported by this experimental fact, in the rest of the paper, our simulations only keep the short trajectories by restricting the absorbing boundary. All the simulation results in the main body of this paper are performed for the case of the CO molecule aligned parallel to the incident laser field. Results for other angles are presented in Appendix B.

III. EFFECT OF DCEP ON THE EVEN-TO-ODD RATIO

We first demonstrate the even-to-odd ratio by the TDSE method for CO molecule without and with DCEP potential, presented in Fig. 2 as SAE and SAE + P, respectively. The 10-cycle laser pulse with the wavelength of 800 nm and intensity of $1.5 \times 10^{14} \text{ W/cm}^2$ is adopted. We also display available experimental data reported in Refs. [24,25]. In these experiments, the CO molecules are partially oriented with degrees of orientation ζ of 0.24 [24] and 0.73 [25], but our simulation is for perfect orientation. Therefore, we normalize the experimental even-to-odd ratios by a factor of $1/\zeta^2$ [31].

The theoretical results with and without DCEP, together with normalized experimental data, are shown in Fig. 2.

Dynamic core-electron polarization is usually thought of as a small perturbation, only producing minuscule corrections to the intensity and shape of HHG spectra [22,23,36]. Surprisingly, Fig. 2 shows that DCEP modifies the even-to-odd ratio as much as one order of magnitude, significantly improving its consistency with experimental data. Specifically, when ignoring the DCEP, the even-to-odd ratio is around one order of magnitude larger than unity for all harmonics, except ones around 37 eV. With DCEP, the ratio only varies within the range $\approx [0, 2]$, matching the experimental energy-dependent even-to-odd ratio in both magnitude and shape. Particularly, with increasing harmonic energy, the even-to-odd ratio gradually grows near unity at harmonics around 21–31 eV and then decreases until reaching the minimum near 37 eV. We also observe an agreement at the peak around 28 eV related to the shape resonance phenomenon [46].

We emphasize that the effect of DCEP in the even-to-odd ratio is so pronounced that even if moderate experimental noise is factored in, the agreement with experiments is still undoubtedly superior to the simple SAE approximation. In Appendix B, we also show that DCEP has a measurable effect in the energy-dependent even-to-odd ratio at different orientation angles, in both parallel and perpendicular HHGs. We thus recommend the even-to-odd ratio as a prospective experiment to study DCEP.

This strong DCEP effect can be understood by estimating the molecular dipole in the external field. The adiabatic electric dipole is approximately $\mu_p + \mu_{\text{ind}}$, where μ_p and $\mu_{\text{ind}} = \alpha_{\text{czz}}E(t)$ are respectively the permanent and induced dipoles of the cation. The value $\mu_p = 1.07 \text{ a.u.}$ is obtained by the chemical code GAUSSIAN09 [47] with the DFT method using the unrestricted hybrid B3LYP functional and the aug-cc-pVQZ basis set. In the laser pulse with the intensity of $1.5 \times 10^{14} \text{ W/cm}^2$, i.e., 0.065 a.u., the electric dipole varies between 0.28 and 1.86 a.u. This asymmetry-induced strong variation results in a considerable effect of even and odd harmonics.

IV. DCEP EFFECT ON HARMONIC TIME PROFILE

To explain the prominent manifestation of DCEP in the even-to-odd ratio, we start from the origin of even and odd harmonics. Harmonic generation is a coherent interference of the attosecond bursts emitted periodically with half-cycle time translation [5]. Specifically, the complex spectral amplitude of harmonic with frequency $n\omega_0$ (ω_0 is the fundamental frequency determined by the laser frequency) is defined as $A(n) = A_1(n) - A_2(n)e^{-i\pi n}$, where $A_1(n)$, and $A_2(n)$ are the complex amplitudes of the harmonic emitted from the opposite sites of the CO molecules [24]. As a result, the odd (even) harmonics are caused by the constructive (destructive) interference of the two successive attosecond bursts. Consequently, we can derive the magnitude of the even-to-odd ratio as

$$\eta(n) = 1 - \frac{2\kappa(n)\cos\Delta\phi(n)}{1 + \kappa(n)\cos\Delta\phi(n)}, \quad (6)$$

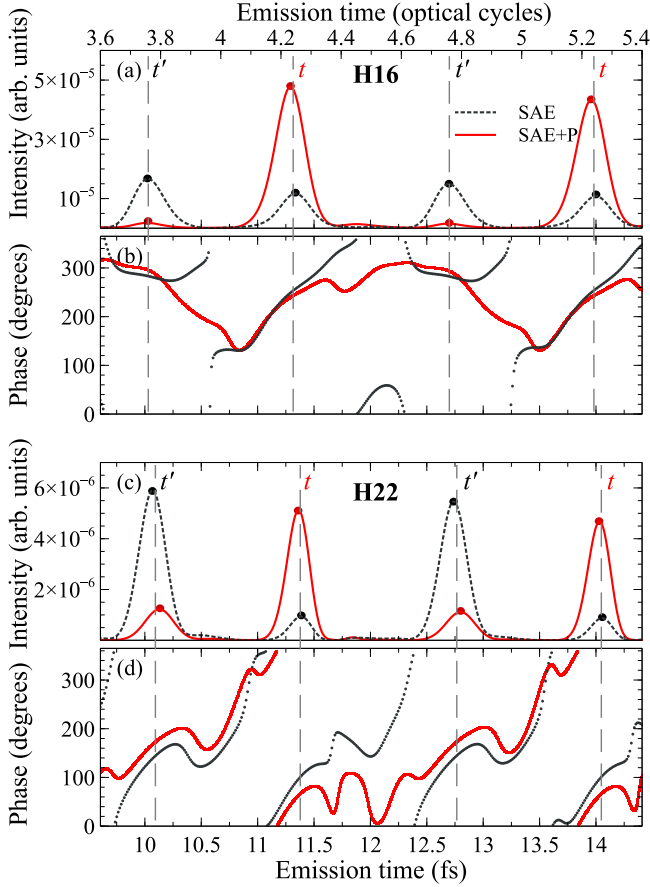


FIG. 3. The time profile intensity [(a), (c)] and phase [(b), (d)] for orders 16 and 22 from theoretical models without (SAE) and with DCEP (SAE + P). The lasers with the same parameters as used in Fig. 2 but with the laser intensity of 1.5×10^{14} W/cm². The red and black circles indicate the peaks of attosecond bursts when ignoring and including DCEP, respectively.

where $\kappa(n) = \frac{2|A_1(n)||A_2(n)|}{|A_1(n)|^2 + |A_2(n)|^2} \in [0, 1]$ is the intensity imbalance, and $\Delta\phi(n)$ is the phase difference of the two adjacent attosecond bursts. The complex spectral amplitude of the attosecond bursts, $A_1(n)$ and $A_2(n)$, can be obtained from induced dipole acceleration obtained from TDSE via the time-frequency transform; see Eq. (5).

By reconstructing the amplitude and phase of the attosecond bursts, we can identify the origin of the DCEP effect on the even-to-odd ratios via their connection with the harmonic time profile. The polar nature of the molecule CO breaks the symmetry between two consecutive laser half-periods, making the destructive interference between two immediate attosecond bursts imperfect. Even though the existence of this symmetry breaking is standard in all theoretical models, its quantitative characteristics strongly depend on the accuracy level of the theory. We show in Fig. 3 the numerical magnitude and phase of the time profile produced with and without DCEP at orders 16 and 22 as examples for low- and high-order harmonics.

As shown in Fig. 3(a) for low-order harmonics, the DCEP enhances the attosecond-burst intensity emitted at the instants $t \approx (1.25 + k)T_0$ (with $k = 1 - 8$ and T_0 is the laser period), while almost eliminates bursts at the half-cycle translation,

$t' \approx (1.76 + k)T_0$. Meanwhile, the intensity imbalance among attosecond bursts produced by the bare SAE is negligible. For high-order harmonic, as in Fig. 3(c), even though SAE displays strong intensity imbalance, the time dependence is opposite to the SAE with DCEP. In both examples, the difference between the two theories is clearly qualitative and can be attributed to the fact that the DCEP significantly enhances the ionization when the electric field points from C to O (called parallel orientation) and depresses the ionization for the inverse case (antiparallel orientation) [17,18]. Matching with classical paths shows that the emission instants t (t') in Fig. 3 correspond to the ionization instants whose electric field has the parallel (antiparallel) orientation. As a result, DCEP amplifies the bursts at t moments and weakens those at t' moments. However, it is surprising that this effect is so strong that it overrides the initial behavior without DCEP. In addition, the DCEP shifts the emission times of the attosecond bursts, for example, for order 22, about 20 as forward at the instants t and about 60 as backward at t' . This observation closely relates to the detuning of emission times of synthesized attosecond pulse for molecular parallel and antiparallel orientations caused by the dynamic deformation of the electronic orbital, as stated in Ref. [22].

Similar to the intensity, the phase also undergoes a significant change as DCEP is taken into account, as shown in Figs. 3(b) and 3(d). This impact is more apparent for high harmonic orders. For low orders, the bursts at t' almost vanish, making the phase difference meaningless. In particular, for order 22, the two bursts at $\approx 4.25T_0$ and $\approx 4.76T_0$ are almost in phase ($\Delta\Phi \approx 44^\circ$) in SAE but out of phase ($\Delta\Phi \approx 107^\circ$) in SAE + P. For order 16, these bursts are still in phase, with the phase differences being about 27° and 49° for SAE and SAE + P, respectively. According to the strong-field approximation [5,48], the phase difference between the two adjacent bursts of a polar molecule consists of three terms representing the phase difference of electron acquired on tunneling ionization, propagation, and recombination steps. The phase differences accumulated during photoionization and photorecombination steps depend on the phase discrepancy between the molecular ground state and the continuum state of a tunneled electron. The phase of the propagation step is accumulated from the ionization to the recombination instants, and relates to the Stark-shifted ion ground state. Moreover, the DCEP deforms the HOMO orbital and changes HOMO energy in the opposite direction for parallel and antiparallel orientations [17,22], and also affects the recombination instants as shown in Figs. 3(a) and 3(c). Consequently, the DCEP can change the phase differences at each step and accordingly the phase differences between the attosecond bursts. Again the effect of DCEP on the harmonic phase is expected, but the surprising result we find is the very high magnitude of this effect. Together with the aforementioned discussion on the harmonic intensity, we can assert that DCEP must be considered not as a correction but on the same level as other terms such as the kinetic energy or the laser potential.

Given the strong effect of DCEP on the harmonic time profile, we now identify the exact mechanism through which DCEP significantly corrects the measurable even-to-odd ratio. In Fig. 4, we present the components of Eq. (6), $\kappa(n)$ and

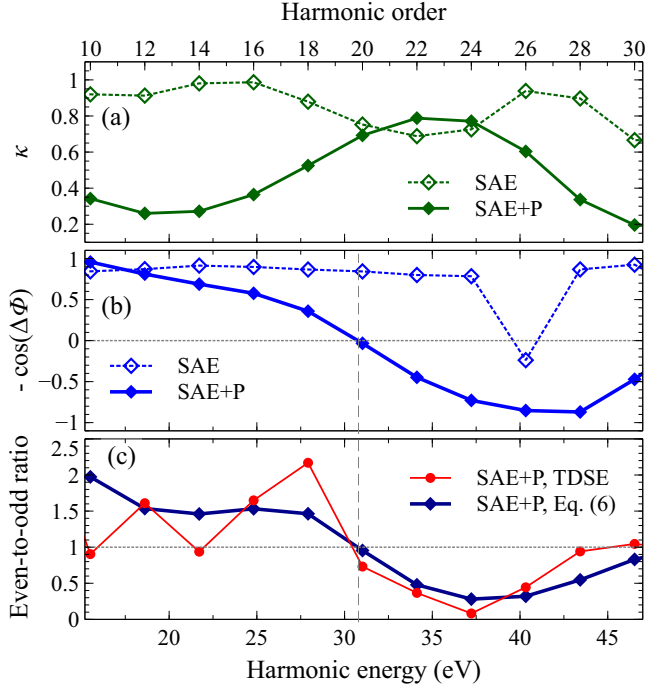


FIG. 4. The illustration of $\kappa(n)$ (a) and $-\cos \Delta\phi(n)$ (b) calculated from the two adjacent attosecond bursts emitted around $4.76T_0$ and $5.25T_0$ for the cases without (SAE) and with DCEP (SAE + P). In panel (c), the even-to-odd ratio calculated by Eq. (6) is compared to the result from TDSE when considering DCEP. The laser parameters are the same as in Fig. 3. The phase difference between the adjacent attosecond bursts and the even-to-odd ratio have similar modulation with harmonic energy.

$-\cos \Delta\phi(n)$ reconstructed from the two adjacent attosecond bursts around $4.76T_0$ and $5.25T_0$. Note that the phase differences here are subtracted by π phase compared with those directly calculated from Gabor transform [Figs. 3(b), 3(d)] due to the half-cycle time translation. Figure 4(a) shows that within the bare SAE, $\kappa(n)$ is close to unity for the most part of the harmonic energy range; while with DCEP, $\kappa(n)$ not only changes its modulation with the harmonic energy but is also significantly reduced in its magnitude. This difference has an important implication to the even-to-odd ratio. The small value of $\kappa(n)$ means a large imbalance in the magnitudes of two consecutive bursts, indicating that besides the region around order 22, for instance, order 16 shown in Fig. 3(a), DCEP almost eliminates the bursts at instants t' . As a result, the even-to-odd ratio produced with DCEP is close to unity as the interference is dominated by bursts at t instants.

In addition to the magnitude imbalance, the bare SAE also incorrectly estimates the phase difference between two consecutive bursts. For $-\cos \Delta\phi(n)$, with increasing the harmonic energy, the value when neglecting DCEP remains mostly positive close to unity (except a sharp dip at order 26). Together with that $\kappa(n) \approx 1$, this means the two consecutive bursts have the same magnitude but opposite phase, resulting in the vanishing odd harmonics and an unphysically large even-to-odd ratio. However, the inclusion of DCEP can correct both the magnitude imbalance and the phase difference, leading to a much more physical even-to-odd ratio.

In Fig. 4(c), we show the even-to-odd ratio reconstructed from components $\kappa(n)$ and $-\cos \Delta\phi(n)$ of adjacent attosecond bursts using Eq. (6) when including DCEP, which agrees well with the simulated data from TDSE both in magnitude and shape. For low harmonic energy, the fluctuation of the simulated from TDSE is not captured by the reconstruction from Eq. (6) since this formula simply utilizes only two adjacent out of a series of attosecond bursts; however, their typical magnitudes are consistent with each other. Interestingly, Figs. 4(b) and 4(c) reveal that $-\cos \Delta\phi(n)$ and the even-to-odd ratio have the same modulation with harmonic energy. The turning point of the even-to-odd ratio from >1 to <1 exactly matches the turning point of $-\cos \Delta\phi(n)$ from positive to negative, as can be understood from Eq. (6). Remarkably, this turning point is confirmed experimentally (see Fig. 2 at around 31 eV), implying that other corrections to the theory might only be of high orders. Following this argument, we emphasize that the analogous turning point of $-\cos \Delta\phi(n)$ is absent in the bare SAE, consistent with the observation that the even-to-odd ratio produced by bare SAE has not only the wrong magnitude scale but also incorrect shape compared to experiments. Our finding complements the DCEP effect on the harmonic phase besides the knowledge on the harmonic intensity found in previous studies [22,23,33,36]. We thus recommend that the basic theoretical framework for polar molecules should be SAE + P (instead of SAE) with the effect of dynamic core polarization calculated unperturbatively.

V. CONCLUSION

In this paper, we have theoretically investigated the even-to-odd ratio of CO molecule by solving the TDSE in the framework of SAE approximation including DCEP. We demonstrate the remarkable influence of the multielectron effect via DCEP on the even-to-odd ratio of CO molecule. Without DCEP, the even-to-odd ratio is much larger than unity, in contrast to the case of including DCEP, where the even-to-odd ratio is close to unity, significantly improving the agreement with available experimental data.

Furthermore, we also explicitly show that the DCEP significantly imprints in the harmonic time profile in both intensities and phases, which directly causes the DCEP signature in an even-to-odd ratio. Our finding complements the understanding of the DCEP effect on the harmonic phase besides the harmonic intensity found in previous studies. We emphasize that the role of DCEP in the even-to-odd ratio is nonperturbative and should be included in the standard theory.

ACKNOWLEDGMENTS

We would like to thank the anonymous referees for the useful comments and suggestions on explaining the DCEP effect on the even-to-odd ratio. We are funded by Vietnam National Foundation for Science and Technology Development (NAFOSTED) under Grant No. 103.01-2020.57. K.-N.H.N. was funded by Vingroup JSC and supported by the Master, Ph.D. Scholarship Programme of Vingroup Innovation Foundation (VINIF), Institute of Big Data, Code No. VINIF.2021.TS.064. This work was carried out by the

high-performance cluster at Ho Chi Minh City University of Education, Vietnam.

APPENDIX A: STABILITY OF EVEN-TO-ODD RATIO

In this Appendix, we prove that removing the long trajectories leads to smooth even-to-odd ratios that are relatively independent of the laser intensities and wavelengths. First, we simulate the case of CO molecular orientation $\theta = 0^\circ$ where only parallel HHG is generated. The simulated odd and even HHG spectra, and even-to-odd ratios are presented in Fig 5.

Figures 5(a) and 5(b) compare the separated odd- and even-harmonic spectra when considering full trajectories (dashed lines) and only the short ones (solid lines). The laser wavelength and intensity are respectively 800 nm and $1.8 \times 10^{14} \text{ W/cm}^2$. The DCEP effect is included for simulating HHG. Figures 5(a) and 5(b) reveal that with full trajectories, except the cutoff region, the intensities of both even- and odd-harmonic spectra strongly fluctuate, thus leading to the oscillation of the energy-dependent even-to-odd ratio, as shown by the blue dashed line in Fig. 5(c). This fluctuation can be attributed to the interference of long and short trajectories in each optical half-cycle of the laser pulse.

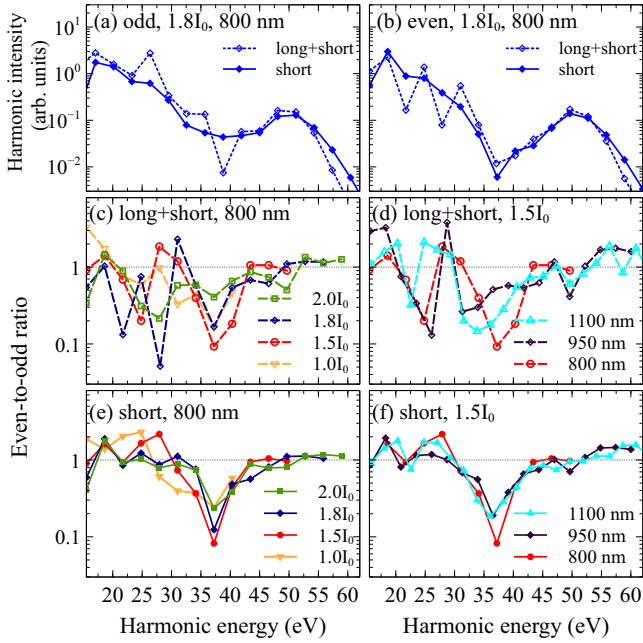


FIG. 5. The separated odd- and even-harmonic spectra [(a), (b)] and the even-to-odd ratios when considering both long and short [(c), (d)], or only short [(e), (f)] trajectories of ionized electrons. In panels (c)–(f), the horizontal dotted gray lines show the even-to-odd ratio equals one. The laser parameters are wavelength of 800 nm and various intensities [(c), (e)]; and intensity of $1.5 \times 10^{14} \text{ W/cm}^2$ and various wavelengths [(d), (f)]. The notation I_0 in the figures stands for $1.0 \times 10^{14} \text{ W/cm}^2$. The molecular orientation angle is 0° . The DCEP effect is included. The elimination of long trajectories smooths the odd- and even-harmonic spectra and the even-to-odd ratios. Moreover, the even-to-odd ratios are stable with changing laser intensities (e) and wavelengths (f).

Only for the harmonics at the cutoff where these two kinds of trajectories are merged, the smooth modulation is observed in the HHG [Figs. 5(a) and 5(b)] and in the even-to-odd ratio [Fig. 5(c)] (as opposed to the rapid oscillating HHG and even-to-odd ratio at low harmonic orders when the long and short trajectories are widely separated). Therefore, avoiding the quantum path interference by removing the long trajectories makes the odd and even spectra [Figs. 5(a) and 5(b)], as well as the even-to-odd ratio [blue solid line in Fig. 5(e)], much smoother. For comparison, we also present the even-to-odd ratio with full trajectories when varying the laser intensities (with the fixed wavelength of 800 nm) shown in Fig. 5(c), and wavelengths (with the fixed intensity $1.5 \times 10^{14} \text{ W/cm}^2$) shown in Fig. 5(d) within the tunneling ionization regime. The results indicate that the fluctuation of the even-to-odd ratio occurs disorderly with the changing of laser parameters. However, it is interesting that when restricted to only short electron trajectories, the even-to-odd ratio is almost insensitive to the laser intensities [Fig. 5(e)] and the wavelengths [Fig. 5(f)]. Our statement is supported by available experimental data showing relatively similar even-to-odd measurements for the CO molecule at different laser intensities (see Fig. 2).

We also examine the stability of the even-to-odd ratio for other molecular orientations and obtain similar results. Macroscopically, this stability ensures that features of the even-to-odd ratio still persist after integration over the laser-focus volume. Therefore, the even-to-odd ratio can be used as a tool to extract molecular asymmetry such as geometric structure or permanent dipole of polar molecules.

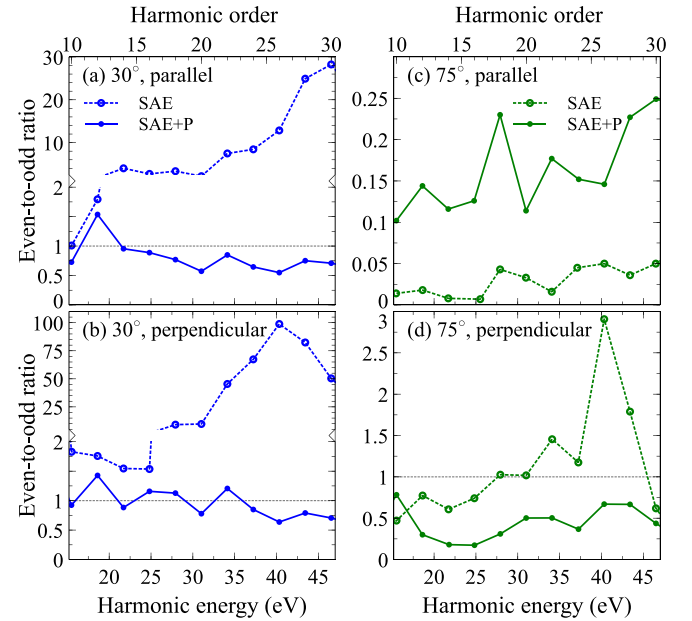


FIG. 6. The simulated even-to-odd ratios for parallel (upper panels) and perpendicular (lower panels) HHG spectra from CO molecules without (SAE) and with the DCEP effect (SAE + P) in the case of orientation angles of 30° [(a), (b)] and 75° [(c), (d)]. The 800-nm laser pulse with the intensity of $1.5 \times 10^{14} \text{ W/cm}^2$ is used. The DCEP affects both the magnitude and shape of the even-to-odd ratio of parallel and perpendicular HHGs.

APPENDIX B: ORIENTATION ANGLES OTHER THAN 0°

Besides the case of $\theta = 0^\circ$ presented in Sec. III, we study the signature of DCEP in the even-to-odd ratio for other orientation angles, where HHG with both parallel and perpendicular polarizations are generated. Figure 6 shows the even-to-odd ratios for the cases of $\theta = 30^\circ$ and $\theta = 75^\circ$ as representatives. The results show that except $\theta = 90^\circ$ whose parallel and perpendicular HHGs contain respectively purely odd and purely even harmonics [33,49,50], the DCEP strongly affects the energy-dependent even-to-odd ratio in both magnitude and shape (one to two orders of magnitude); see Fig. 6. In particular, for small alignment angles with $\theta < 60^\circ$ [Figs. 6(a) and 6(b)], the even-to-odd ratio with DCEP is mostly around unity, while it is much greater than unity when omitting DCEP. It means that the even harmonics substantially predominate the odd ones for the bare SAE, but

they are comparable in the whole plateau when including DCEP.

For the orientation angle $\theta = 75^\circ$ shown in Fig. 6(c), the even-to-odd ratio of parallel HHG in both cases SAE and SAE + P is less than unity, which implies that the intensity of the odd harmonic orders is much greater than that of the even ones. For the bare SAE, the even-to-odd ratio is extremely low since the even harmonic orders almost vanish. In other words, when the orientation angle approaches 90° , the DCEP slows down the diminishing of even orders for parallel HHG.

For the perpendicular HHG at $\theta = 75^\circ$ presented in Fig. 6(d), the even-to-odd ratio of the bare SAE is greater than unity for high-order harmonics, meaning the intensity of even harmonic orders predominates the odd ones. Meanwhile, the odd harmonics still dominate the even ones when including DCEP. In this case, the intensity of the odd harmonic orders with DCEP decreases slower than those without DCEP.

-
- [1] F. Krausz and M. Ivanov, *Rev. Mod. Phys.* **81**, 163 (2009).
 - [2] L. Holmegaard, J. L. Hansen, L. Kalhøj, S. L. Kragh, H. Stapelfeldt, F. Filsinger, J. Küpper, G. Meijer, D. Dimitrovski, M. Abu-Samha, C. P. J. Martiny, and L. B. Madsen, *Nat. Phys.* **6**, 428 (2010).
 - [3] T. Popmintchev, M.-C. Chen, D. Popmintchev, P. Arpin, S. Brown, S. Ališauskas, G. Andriukaitis, T. Balāiunas, O. D. Mücke, A. Pugzlys, A. Baltuška, B. Shim, S. E. Schrauth, A. Gaeta, C. Hernández-García, L. Plaja, A. Becker, A. Jaron-Becker, M. M. Murnane, and H. C. Kapteyn, *Science* **336**, 1287 (2012).
 - [4] P. B. Corkum, *Phys. Rev. Lett.* **71**, 1994 (1993).
 - [5] M. Lewenstein, P. Balcou, M. Y. Ivanov, A. L'Huillier, and P. B. Corkum, *Phys. Rev. A* **49**, 2117 (1994).
 - [6] N. I. Shvetsov-Shilovski, D. Dimitrovski, and L. B. Madsen, *Phys. Rev. A* **85**, 023428 (2012).
 - [7] N. I. Shvetsov-Shilovski, M. Lein, and L. B. Madsen, *Phys. Rev. A* **98**, 023406 (2018).
 - [8] M. Nurhuda and F. H. M. Faisal, *Phys. Rev. A* **60**, 3125 (1999).
 - [9] W. Becker, F. Grasbon, R. Kopold, D. B. Milošević, G. G. Paulus, and H. Walther, *Adv. At. Mol. Opt. Phys.* **48**, 35 (2002).
 - [10] D. Bauer and P. Koval, *Comput. Phys. Commun.* **174**, 396 (2006).
 - [11] A. Gordon, F. X. Kärtner, N. Rohringer, and R. Santra, *Phys. Rev. Lett.* **96**, 223902 (2006).
 - [12] J. Wu, L. P. H. Schmidt, M. Kunitski, M. Meckel, S. Voss, H. Sann, H. Kim, T. Jahnke, A. Czasch, and R. Dörner, *Phys. Rev. Lett.* **108**, 183001 (2012).
 - [13] P. Sándor, A. Sissay, F. Mauger, P. M. Abanador, T. T. Gorman, T. D. Scarborough, M. B. Gaarde, K. Lopata, K. J. Schafer, and R. R. Jones, *Phys. Rev. A* **98**, 043425 (2018).
 - [14] D. Dimitrovski, J. Maurer, H. Stapelfeldt, and L. B. Madsen, *Phys. Rev. Lett.* **113**, 103005 (2014).
 - [15] Y. L. Wang, S. G. Yu, X. Y. Lai, X. J. Liu, and J. Chen, *Phys. Rev. A* **95**, 063406 (2017).
 - [16] Z. Zhao and T. Brabec, *J. Mod. Opt.* **54**, 981 (2007).
 - [17] B. Zhang, J. Yuan, and Z. Zhao, *Phys. Rev. Lett.* **111**, 163001 (2013).
 - [18] V.-H. Hoang, S.-F. Zhao, V.-H. Le, and A.-T. Le, *Phys. Rev. A* **95**, 023407 (2017).
 - [19] S. Ohmura, T. Kato, H. Ohmura, S. Koseki, and H. Kono, *J. Phys. B: At. Mol. Opt. Phys.* **53**, 184001 (2020).
 - [20] M. Abu-samha and L. B. Madsen, *Phys. Rev. A* **101**, 013433 (2020).
 - [21] G. Shi, Y. Xiang, P. Wang, Z. Wang, S. Sun, Z. Liu, and B. Hu, *J. Mod. Opt.* **68**, 10 (2021).
 - [22] B. Zhang, J. Yuan, and Z. Zhao, *Phys. Rev. A* **90**, 035402 (2014).
 - [23] C.-T. Le, V.-H. Hoang, L.-P. Tran, and V.-H. Le, *Phys. Rev. A* **97**, 043405 (2018).
 - [24] E. Frumker, N. Kajumba, J. B. Bertrand, H. J. Wörner, C. T. Hebeisen, P. Hockett, M. Spanner, S. Patchkovskii, G. G. Paulus, D. M. Villeneuve, A. Naumov, and P. B. Corkum, *Phys. Rev. Lett.* **109**, 233904 (2012).
 - [25] P. M. Kraus, D. Baykusheva, and H. J. Wörner, *Phys. Rev. Lett.* **113**, 023001 (2014).
 - [26] E. Frumker, C. T. Hebeisen, N. Kajumba, J. B. Bertrand, H. J. Wörner, M. Spanner, D. M. Villeneuve, A. Naumov, and P. B. Corkum, *Phys. Rev. Lett.* **109**, 113901 (2012).
 - [27] Y. J. Chen, L. B. Fu, and J. Liu, *Phys. Rev. Lett.* **111**, 073902 (2013).
 - [28] W. Y. Li, S. J. Yu, S. Wang, and Y. J. Chen, *Phys. Rev. A* **94**, 053407 (2016).
 - [29] Y. Chen and B. Zhang, *Phys. Rev. A* **84**, 053402 (2011).
 - [30] B. Zhang, S. Yu, Y. Chen, X. Jiang, and X. Sun, *Phys. Rev. A* **92**, 053833 (2015).
 - [31] S. J. Yu, W. Y. Li, Y. P. Li, and Y. J. Chen, *Phys. Rev. A* **96**, 013432 (2017).
 - [32] N.-L. Phan, K.-N. H. Nguyen, C.-T. Le, D. D. Vu, K. Tran, and V.-H. Le, *Phys. Rev. A* **102**, 063104 (2020).
 - [33] N.-L. Phan, C.-T. Le, V.-H. Hoang, and V.-H. Le, *Phys. Chem. Chem. Phys.* **21**, 24177 (2019).
 - [34] E. Runge and E. K. U. Gross, *Phys. Rev. Lett.* **52**, 997 (1984).
 - [35] J. Zanghellini, M. Kitzler, T. Brabec, and A. Scrinzi, *J. Phys. B: At. Mol. Opt. Phys.* **37**, 763 (2004).
 - [36] C.-T. Le, D.-D. Vu, C. Ngo, and V.-H. Le, *Phys. Rev. A* **100**, 053418 (2019).

- [37] M. Abu-samha and L. B. Madsen, *Phys. Rev. A* **81**, 033416 (2010).
- [38] S.-F. Zhao, C. Jin, A.-T. Le, T. F. Jiang, and C. D. Lin, *Phys. Rev. A* **81**, 033423 (2010).
- [39] K. Siegbahn, *J. Electron Spectros. Relat. Phenom.* **5**, 3 (1974).
- [40] J. Heslar, D. Telnov, and S.-I. Chu, *Phys. Rev. A* **83**, 043414 (2011).
- [41] C. C. Chirilă, I. Dreissigacker, E. V. van der Zwan, and M. Lein, *Phys. Rev. A* **81**, 033412 (2010).
- [42] H. Yu and A. D. Bandrauk, *Phys. Rev. A* **56**, 685 (1997).
- [43] V. V. Strelkov, M. A. Khokhlova, A. A. Gonoskov, I. A. Gonoskov, and M. Y. Ryabikin, *Phys. Rev. A* **86**, 013404 (2012).
- [44] S. Yu, B. Zhang, Y. Li, S. Yang, and Y. Chen, *Phys. Rev. A* **90**, 053844 (2014).
- [45] B. Zhang and M. Lein, *Phys. Rev. A* **100**, 043401 (2019).
- [46] E. W. Plummer, T. Gustafsson, W. Gudat, and D. E. Eastman, *Phys. Rev. A* **15**, 2339 (1977).
- [47] M. J. Frisch, G. W. Trucks, H. B. Schlegel, G. E. Scuseria, M. A. Robb, J. R. Cheeseman, G. Scalmani, V. Barone, B. Mennucci, G. A. Petersson, H. Nakatsuji, M. Caricato, X. Li, H. P. Hratchian, A. F. Izmaylov, J. Bloino, G. Zheng, J. L. Sonnenberg, M. Hada, M. Ehara, K. Toyota, R. Fukuda, J. Hasegawa, M. Ishida, T. Nakajima, Y. Honda, O. Kitao, H. Nakai, T. Vreven, J. A. Montgomery, J. E. Peralta, F. Ogliaro, M. Bearpark, J. J. Heyd, E. Brothers, K. N. Kudin, V. N. Staroverov, R. Kobayashi, J. Normand, K. Raghavachari, A. Rendell, J. C. Burant, S. S. Iyengar, J. Tomasi, M. Cossi, N. Rega, J. M. Millam, M. Klene, J. E. Knox, J. B. Cross, V. Bakken, C. Adamo, J. Jaramillo, R. Gomperts, R. E. Stratmann, O. Yazyev, A. J. Austin, R. Cammi, C. Pomelli, J. W. Ochterski, R. L. Martin, K. Morokuma, V. G. Zakrzewski, G. A. Voth, P. Salvador, J. J. Dannenberg, S. Dapprich, A. D. Daniels, Ö. Farkas, J. B. Foresman, J. V. Ortiz, J. Cioslowski, and D. J. Fox, Gaussian 09 Revision A.2, 2009
- [48] A.-T. Le, H. Wei, C. Jin, and C. D. Lin, *J. Phys. B: At. Mol. Opt. Phys.* **49**, 053001 (2016).
- [49] H. Hu, N. Li, P. Liu, R. Li, and Z. Xu, *Phys. Rev. Lett.* **119**, 173201 (2017).
- [50] H. Yin, D. Liu, and F. Zeng, *Appl. Phys. Lett.* **119**, 151105 (2021).